

Bonding and abrasion resistance of geopolymeric repair material made with steel slag

Shuguang Hu ^a, Hongxi Wang ^{a,b,*}, Gaozhan Zhang ^a, Qingjun Ding ^a

^a School of Materials Science and Engineering, Wuhan University of Technology, Wuhan 430070, China

^b Key Laboratory of Nonferrous Materials and Processing Technology, Guilin University of Technology, Ministry of Education, Guilin 541004, China

Received 30 April 2006; received in revised form 23 March 2007; accepted 11 April 2007

Available online 18 April 2007

Abstract

Three repair materials were prepared using cement-based, geopolymeric, or geopolymeric containing steel slag binders. Their mechanical performances such as compressive strength, bond strength and abrasion resistance were examined experimentally. The test results showed that the geopolymeric materials had better repair characteristics than cement-based repair materials, and the addition of steel slag could improve significantly the abrasion resistance of geopolymeric repair. By means of scanning electron microscopy (SEM) it can also be concluded that the steel slag was almost fully absorbed to take part in the alkali-activated reaction and be immobilized into the amorphous aluminosilicate geopolymer matrix.

© 2007 Elsevier Ltd. All rights reserved.

Keywords: Geopolymer; Steel slag; Repair material

1. Introduction

Pioneered by Davidovits in the late 1970s [1], geopolymers are a novel class of materials that are formed by the polymerization of silicon, aluminum, and oxygen species to form an amorphous three-dimensional framework structure. Geopolymeric reactants could range from kaolinite or metakaolin to a group of materials containing rich SiO₂ and/or Al₂O₃ oxides, e.g., fly ash, slag, construction waste and natural minerals. As we know, chemical bonds of Si–O and Al–O are among the most stable covalent bonds in nature. In addition, the polycondensation degree of geopolymer is much higher than cement-based materials [2]. Therefore, geopolymer materials possess many advanced properties such as the ease with which it can be recycled, excellent compressive and bond strength [3], long-term

durability, better acid resistance [4]. Besides, it is also a “Green Material” for its low manufacturing energy consumption and low waste gas emission [5]. Because of these prominent characteristics, geopolymer was considered as one of the potential candidates to solve the conflict between social development and environmental pollution from binder [6]. However, little work has been reported about geopolymeric repair materials.

On the other hand, steel slag is a by-product of the conversion of iron to steel, which results in large environmental pollution in China. Because olivine, merwinite, C₃S, C₂S, C₄AF, C₂F, RO phase (CaO–FeO–MnO–MgO solid solution) and free-CaO are common minerals in steel slag, the presence of C₃S, C₂S, C₄AF, C₂F endows steel slag its cementitious properties. But the reactivity of steel slag is small because of its thermal history, as a consequence, its large application in the concrete and cement as a kind of additive is almost impossible. However, the authors [7] investigated water-glass-activated steel slag/blast furnace slag (BFS) and concluded that the alkali-activated mixture possess much higher strengths than Grade-425 ordinary Portland cement.

* Corresponding author. Address: School of Materials Science and Engineering, Wuhan University of Technology, Wuhan 430070, China. Tel.: +86 27 87668602; fax: +86 27 87392350.

E-mail address: dingwang@whut.edu.cn (H. Wang).

Good bond and wear resistance are the two main requirements for successful repair [8,9]. The geopolymers possess good bond strength and the steel slag is good wear resistance because of the Fe phase existing in it. In this paper, we focused on reporting the influences of the steel slag to the properties of geopolymeric repair materials.

2. Experimental

2.1. Materials

Metakaolin used in this study was obtained by calcining kaolin at 750 °C for 6 h. It was used for reactive Si–Al cementitious materials. Steel slag powder used in this study was obtained from Wuhan Iron and Steel Corp., Wuhan, China. Solids from different batches were bulk mixed prior to their use and the compositions as determined by fusion analysis using a Siemens SRS3000 sequential X-ray fluorescence (XRF) spectrometer are listed in Table 1. Their particle size distribution is shown in Table 2. The cement used as the control sample was Grade-42.5 ordinary Portland cement. The main component of U-type expansive agent (UEA) is calcium sulphoaluminate.

Analytical grade NaOH and sodium silicate solution with the molar ratio of SiO₂ to Na₂O of 3.19 were used as reagents, respectively. Distilled water was used throughout.

Table 1
Composition of kaolinite as determined by fusion and XRF analysis (wt.%)

Element as oxide	Kaolinite (wt.%)	Steel slag (wt.%)	Cement (wt.%)
SiO ₂	53.1	15.0	22.2
Al ₂ O ₃	30.9	6.7	4.8
CaO	0.1	44.2	62.5
Fe ₂ O ₃	1.6	15.4	6.2
MgO	0.3	10.9	1.5
TiO ₂	2.0	3.1	
Na ₂ O	0.3	0.2	0.3
K ₂ O	0.1	0.1	
SO ₃	0	0.7	1.1
f-CaO		1.7	
Fe		1.0	
Other minor oxides	0.3	0.4	
Loss on ignition	11.3	0.6	1.4
Total	100.00	100.00	100.00

Table 2
Particle size distribution of raw materials

Diameters (μm)	0.5	1	3	5	10	15	20	30	40
Kaolinite	2.85	20.3	65.7	89.9	97.3	99.3	99.6	99.8	100
Steel slag	0	0.67	15.9	40.1	72.9	89.6	92.1	94.6	100

Table 3

The mixture proportion of the repair materials (wt.%)

Mixture number	Water:cement:UEA	Metakaolin	Steel slag	Water-glass
Cement repair (CR)	0.4:0.95:0.05			
Geopolymeric repair (GR)		1		0.56
Geopolymeric repair with steel slag (GRS)		0.8	0.2	0.56

2.2. Methods

2.2.1. Mixture proportion

In this study, three kinds of repair materials were prepared. The details of mixture proportion, compressive strength of the repair materials and old substrate are given in Table 3. The NaOH and sodium silicate solution, and water were first mixed in a beaker to form the alkali-activated solution (water-glass) that the SiO₂/Na₂O molar ratio was 1.14 and the mass concentration was 38%, and cooled up to room temperature. Powder metakaolin and steel slag was mixed for 2 min, and then they were added into the cooled alkaline solution and mixed for another 3 min.

2.2.2. Compressive strength testing

The fresh geopolymer with or without steel slag and cement pastes were rapidly poured into steel moulds of dimension with 40 × 40 × 40 mm. The specimens were demoulded after 24 h curing at 20 ± 0.5 °C and 95% relative humidity, and then submitted to compressive strength test at curing ages of 8 h, 1 d, 3 d, 7 d, 28 d.

2.2.3. Bond strength testing

Samples for interfacial bonding strength determination between the new repair materials and the old concrete substrate were prepared as shown in Fig. 1. The old substrates with the proportion of water:cement:sand (0.4:1:3) were cast as indicated in Fig. 1, then cured at 20 °C and 95% relative humidity for 28 d. As indicated in Fig. 1, freshly prepared repair layer (5 mm thick) was then glued to the middle of the old substrates for the bond strength test.

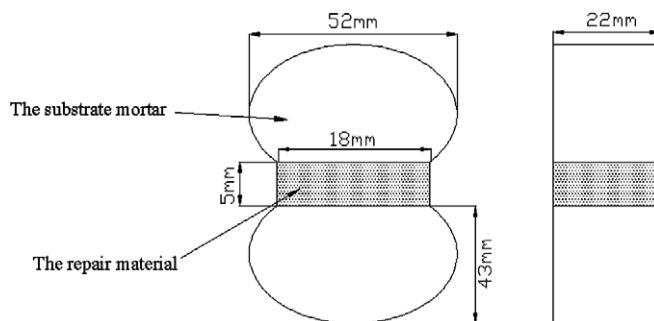


Fig. 1. Test set-up of the bond strength between the substrate mortar-repair materials in sandwich specimens.

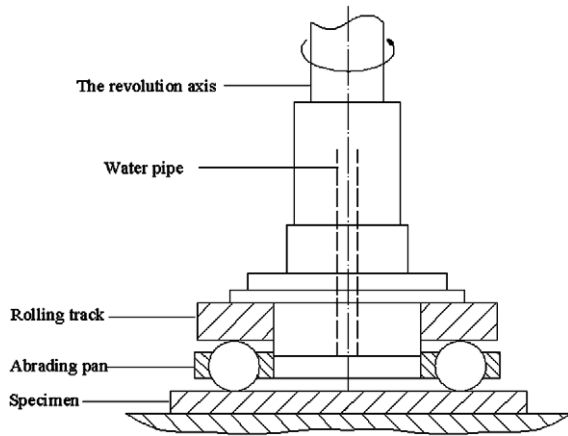


Fig. 2. The sketch of the test set-up for abrasion resistance.

When the cement repair material was glued, the resultant sandwich specimen was named C_b . When the geopolymer was glued, the resultant sandwich specimen was named G_b . When the geopolymer with steel slag was glued, the resultant sandwich specimen was named GS_b .

2.2.4. Abrasion resistance

Abrasion resistance was tested in accordance with GB16925-1997, which was published by the Chinese Building Material Industry, which the test set-up shown in Fig. 2. The 100 mm diameter cylinders with a 2:1 diameter-to-length ratio were fixed in the holding device of the abrasion machine and a load of 154 ± 2.5 N was applied. The grinding machine was then put in motion at a speed of 1000 rpm. Each specimen was abraded for 5 min and the depth of grinding trace on the specimen surface was measured at the fifth minute. The results for the grade of abrasion resistance were evaluated using the following formula:

$$I_a = \sqrt{R/P} \quad (1)$$

where I_a is the grade of abrasion resistance; R is the number of revolution of grinding machine in 1000 rpm; P is the depth of grinding trace in mm.

2.2.5. Microstructure analysis

Scanning electron microscopy (SEM) was used to investigate the images of the geopolymeric repair materials with steel slag. The sandwich samples used in the bond strength testing were destroyed and then lightly polished at the cracking before micrographs were taken for SEM test.

3. Results and discussion

3.1. Compressive strength

The results of the 8 h, 1 d, 3 d, 7 d, 28 d compressive strength tests on the various repair materials are summarized in Table 4. From Table 4, it was found that the compressive strength of the cement repair material is lower

Table 4

Compressive strength of the repair materials at various ages

Mixture number	Compressive strength (MPa)				
	8 h	1 d	3 d	7 d	28 d
Cement repair (CR)	–	8.7	23.2	33.1	46.1
Geopolymeric repair (GR)	10.4	17.2	30.4	37.8	40.9
Geopolymeric repair with steel slag (GRS)	14.3	22.1	35.6	40.4	44.5

than that of the geopolymeric repair material with or without steel slag at the 8 h, 1 d, 3 d, 7 d, but at 28-d, the results were the opposite. The higher early compressive strength of geopolymeric repair materials could be attributed to their activated character. Comparing GRS with GR, it was found that the 8 h, 1 d, 3 d, 7 d, 28 d compressive strengths increased 43%, 28%, 17%, 6.9%, 7.6%, respectively. The addition of steel slag could accelerate the setting time and significantly improve compressive strength, which could be due to its latent hydraulic cementitious character.

3.2. Bond strength

The results of the 8 h, 1 d, 3 d, 7 d, 28 d bond strength tests on the various repair materials are summarized in Table 5. As shown in Table 5, the bond strengths of G_b and GS_b at 1 d were both higher than of C_b at 7 d. Similarly, the bond strength of G_b and GR_b at 3 d were both higher than of C_b . The bond strength of GS_b at 3 d was 2.6% and 600% higher than of G_b , C_b , respectively. Similarly, the bond strength of GS_b at 28 d was 4.4% and 55.9% higher than of G_b , C_b , respectively. It could be seen that the geopolymeric materials possessed better bonding character than cement materials.

The noticeable increase in bond strength was due to reasons: the improvement of the interfacial transition zone between the old substrate and repair materials and the increasing of the tensile strength of repair material. Fig. 3 shows the failure modes of specimens for bond strength test. Failures occurred in the three different regions: (1) in the interfacial transition zone between the substrate and repair materials, named mode A; (2) in the repair materials, named mode B; and (3) throughout the substrate and the repair materials, named mode C. The failure mode of the repair materials at different age can be seen in Table 5. The failure mode of cement repair materials was mainly mode A. The failure mode of the geopolymeric repair materials was mainly mode B at the age of 8 h, 1 d, and

Table 5

Bond strength and failure mode of the repair materials

Mixture number	Bond strength (MPa)					Failure mode				
	8 h	1 d	3 d	7 d	28 d	8 h	1 d	3 d	7 d	28 d
C_b	–	–	0.34	1.17	1.95	B	A	A	A	A
G_b	0.42	1.23	2.34	2.43	2.91	B	B	C	C	C
GS_b	0.45	1.27	2.40	2.47	3.04	B	B	C	C	C

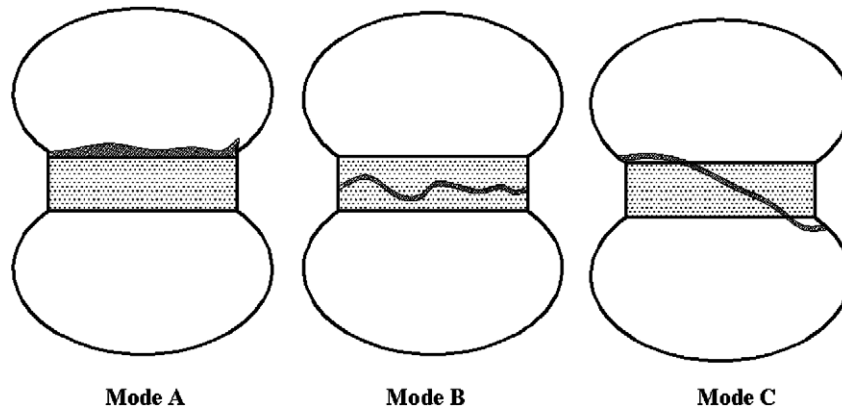


Fig. 3. Failure modes of specimens in bond strength test.

was mainly mode C at the age of 3 d, 7 d, 28 d. Failure mode A was attributive to the week interface, and failure mode B or C was attributive to the week tensile strength of the geopolymeric repair materials or the old substrate. It could be inferred that the interfacial transition zone between the old substrate and geopolymeric repair materials could be improved because of the reaction between the alkali activator and the surface product of the old substrate, thus leading to an even denser interface zone with better bond strength.

3.3. Abrasion resistance

The abrasion resistance of repair materials was determined at the ages of 3, 7, 28, 56 and 90 d. It was measured in term of depth of wear as shown in Table 6. It was observed that depth of wear decreased with the increase of the age for the repair materials. Comparing P_G with P_C , the P values at 3, 7, 28, 56 and 90 d decreased 48%, 44%, 29%, 28%, 29%, respectively. Comparing P_{GS} with

Table 6
Depth of grind track of the repair materials

Mixture number	P (mm)				
	3 d	7 d	28 d	56 d	90 d
Cement repair (P_C)	6.41	5.42	4.21	4.01	3.89
Geopolymeric repair (P_G)	3.32	3.03	2.98	2.87	2.76
Geopolymeric repair with steel slag (P_{GS})	3.02	2.76	2.34	2.23	2.14

P_G , the P values at 3, 7, 28, 56 and 90 d decreased 9%, 8.9%, 21.4%, 22.2%, 22.5%, respectively. This showed that the depth of wear for geopolymeric repair materials was smaller than for the cement repair materials, which means that the abrasion resistance for geopolymeric repair materials was better. The decreasing extent for the P_G and P_{GS} value from 3 d to 28 d is smaller than for the P_C , which is similar to the relation in their compressive strengths. This is mainly because the abrasion resistance of repair materials is determined by the density of the structure. The geo-

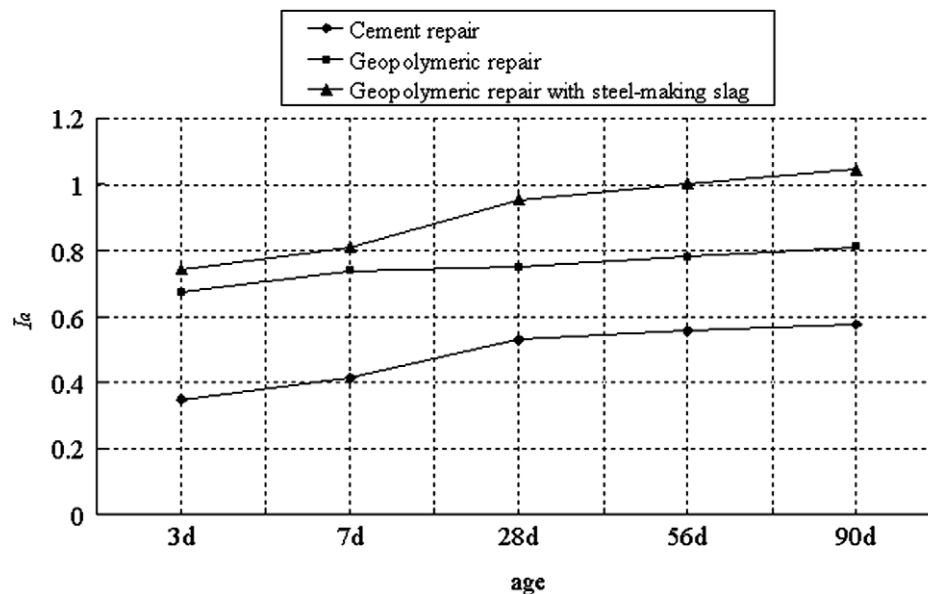


Fig. 4. The grade of abrasion resistance of the repair materials at various ages.

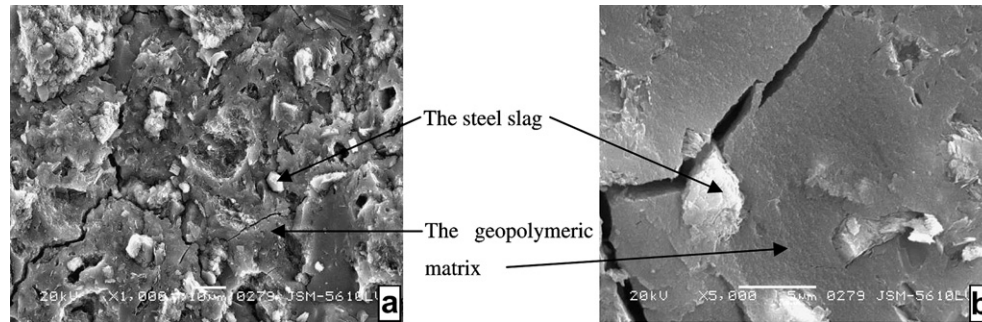


Fig. 5. SEM tested of geopolymeric repair with steel-making slag at 1 d, 20 ± 0.5 °C, 95% relative humidity: (a) 1000 \times and (b) 5000 \times .

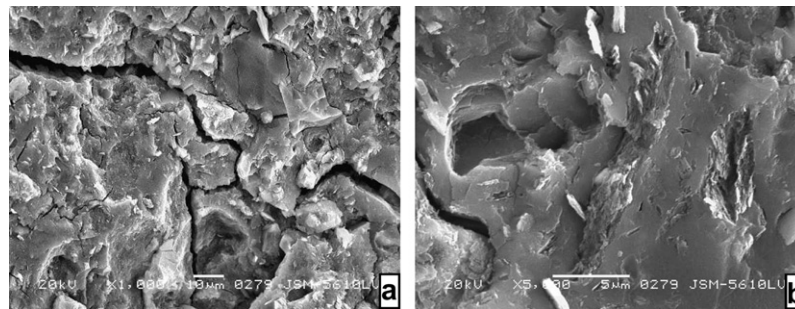


Fig. 6. SEM tested of geopolymeric repair with steel-making slag at 28 d, 20 ± 0.5 °C, 95% relative humidity: (a) 1000 \times and (b) 5000 \times .

polymeric repair materials could form a dense structure earlier than the cement repair materials.

The calculated value about the grade of abrasion resistance for the repair materials at various ages is plotted in Fig. 4. Fig. 4 shows the grade of abrasion resistance increased with the increase of the age for the repair materials. It could be seen that the I_a for the geopolymeric repair is higher than for the cement repair, but lower than for the geopolymeric repair with steel slag.

3.4. Microstructure analysis

It could be observed in Fig. 4 that the geopolymeric repair with steel slag had the best abrasion resistance, which could be due to the addition of steel slag. Figs. 5 and 6 show some microstructural characteristics of the geopolymeric repair materials with steel slag by means of scanning electron microscopy (SEM) methods.

As can be observed in these figures, the geopolymeric repair materials studied through SEM have quite different microstructure at different ages. At 1 d age, 20 ± 0.5 °C, 95% relative humidity, the resulting material is a porous one (see Fig. 5a). In many cases, a surface reaction is responsible for bonding the undissolved steel slag particles into the final aluminosilicate matrix structure. The reacted steel slag particles appear to be immobilized into the amorphous aluminosilicate matrix (see Fig. 5b). Fig. 6a shows that the geopolymeric repair materials at 28 d age, 20 ± 0.5 °C, 95% relative humidity had more compact structure than the geopolymeric repair materials at 1 d age, 20 ± 0.5 °C, 95% relative humidity. Fig. 6b shows that

the steel slag particles have almost fully reacted with the sodium silicate solution and could not be observed from the SEM, which could be the reason why the compressive and bond strengths are higher at 28 d age.

4. Conclusions

Within the indicated scope of this study, the particular conclusions may be summarized as follows:

1. The compressive strength of the cement repair material is lower than that of the geopolymeric repair material with or without steel slag at the 8 h, 1 d, 3 d, 7 d, but at 28-d, the opposite is true.
2. The geopolymeric repair materials have better repair characteristics than cement-based repair materials. The bond strength of GS_b at 3 d was 2.6% and 600% higher than those of G_b and C_b , respectively. Similarly, the bond strength of GS_b at 28 d was 4.4% and 55.9% higher than those of G_b , C_b , respectively.
3. The geopolymeric repair materials had better abrasion resistance character than the cement repair. The P_G values at 3, 7, 28, 56 and 90 d decreased 48%, 44%, 29%, 28%, 29% than P_C , respectively. The addition of steel slag could improve significantly the abrasion resistance performance of the geopolymeric repair. Comparing P_{GS} with P_G , the P values at 3, 7, 28, 56 and 90 d decreased 9%, 8.9%, 21.4%, 22.2%, 22.5%, respectively.
4. The steel slag was almost fully absorbed to take part in the alkali-activated reaction and be immobilized into the

amorphous aluminosilicate geopolymer matrix by means of scanning electron microscopy (SEM).

Acknowledgements

The authors gratefully acknowledge the key technology R&D program of 10th Five-Year Plan of China for financially supporting the Project No. 2003BA652C and the Opening Fund of Key Laboratory of Nonferrous Materials and Processing Technology.

References

- [1] Davidovits J. Geopolymers and geopolymeric new materials. *J Therm Anal* 1989;35(2):429–41.
- [2] Yang NR. Physical chemistry basis for the formation of alkaline cementitious material. *J Chin Ceram Soc* 1996;24(4):459–65.
- [3] van Jaarsveld JGS, van Deventer JSJ, Lukey GC. The characterisation of source materials in fly ash based geopolymers. *Mater Lett* 2003;57(7):1272–86.
- [4] Phair JW, Van Deventer JSJ. Effect of silicate activator pH on the leaching and material characteristics of waste-based geopolymers. *Miner Eng* 2001;14(3):289–304.
- [5] Xu Hua, Van Deventer JSJ. The geopolymerisation of aluminosilicate minerals. *Int J Miner Process* 2000;59(3):247–66.
- [6] Davidovits J. Method for bonding fiber reinforcement on concrete and steel structures and resultant products, US Patent No. 5925449; 1999.
- [7] Hu SG, Wei JX, Ding QJ. Research on excitation principle of sodium silicate to steel slag cement. *Cement Eng* 2001;5:4–6 [in Chinese].
- [8] Xiong GJ, Cui YQ, Chen LQ, Jiang H. Influence of hydrochloric acid etching on bond strength between concrete substrate and repair materials. *Cem Concr Compos* 2004;26:41–5.
- [9] Siddique R. Performance characteristics of high-volume class F fly ash concrete. *Cem Concr Res* 2004;34:487–93.